Coherent energy scale revealed by ultrafast dynamics of UX_{3} (X = Al, Sn, Ga) single crystals

Saritha K. Nair, J.-X. Zhu, J. L. Sarrao, A. J. Taylor, and Elbert E. M. Chia

Phys. Rev. B **86**, 115103 — Published 4 September 2012

DOI: 10.1103/PhysRevB.86.115103

Coherent energy scale revealed by ultrafast dynamics of UX_3 (X=Al, Sn, Ga) single crystals

Saritha K. Nair,[1] J.-X. Zhu,[2] J. L. Sarrao,[2] A. J. Taylor,[2] and Elbert E. M. Chia[1]

[1]*Division of Physics and Applied Physics, School of Physical and Mathematical Sciences, Nanyang Technological University, Singapore 637371, Singapore*

[2]*Los Alamos National Laboratory, Los Alamos, New Mexico 87545, USA*

(Dated: August 24, 2012)

Temperature dependence of relaxation dynamics of UX_3 (X = Al, Ga, Sn) compounds is studied using time resolved pump-probe technique in the reflectance geometry. For UGa_3, our data are consistent with the formation of a spin density wave SDW gap as evidenced from the quasidivergence of the relaxation time τ near the Néel temperature T_N. For UAl_3 and USn_3, the relaxation dynamics shows a change from single exponential to two exponential behavior below a particular temperature, suggestive of coherence formation of the $5f$ electrons with the conduction band electrons. This particular temperature can be attributed to the spin fluctuation temperature T_{sf}, a measure of the strength of Kondo coherence. Our T_{sf} is consistent with other data such as resistivity and susceptibility measurements. The temperature dependence of the relaxation amplitude and time of UAl_3 and USn_3 were also fitted by the Rothwarf-Taylor model. Our results show ultrafast optical spectroscopy is sensitive to c-f Kondo hybridization in the f-electron systems.

I. INTRODUCTION

The uranium compounds UX_3, where X is a IIIb (Al, Ga, In, Tl) or IVb (Si, Ge, Sn, Pb) element, crystallize in the cubic $AuCu_3$-type structure[1] and have U-U distances (d_{U-U}) much larger than the Hill limit (~ 3.5 Å) for uranium compounds.[2] The different degree of hybridization of the $5f$ electron orbitals with the conduction electron orbitals in these compounds leads to a wide range of magnetic behavior such as Pauli enhanced paramagnetism (UAl_3, USi_3, and UGe_3), antiferromagnetism (UGa_3, UPb_3 and UIn_3), and heavy fermion behavior (USn_3).[1,3,4] Due to the the above-mentioned properties and the availability of high quality crystals, UX_3 compounds are ideal candidates for studying how physical properties and underlying electronic structure are related.

The anomalous behavior of the resistivities of UX_3 compounds can be explained on the basis of spin fluctuations in narrow $5f$ bands.[5,6] A temperature characteristic of the spin fluctuations in the UX_3 compounds is the spin fluctuation temperature, T_{sf}, which expresses the strength of hybridization between f and conduction electrons (c-f hybridization). The degree of hybridization is related to the degree of delocalization of the f-electrons. A high value of T_{sf} corresponds to more easily hybridized (delocalized) electrons. Above T_{sf}, f-electrons are localized; whereas below T_{sf}, there is quasiparticle coherence from the hybridization between f-electrons and conduction electrons, *i.e.*, f-electrons now become more delocalized (or itinerant). The effective hybridization below T_{sf} leads to changes in measured physical properties. For example, the electrical resistivity changes from a T-linear law above T_{sf} to a T-quadratic law below this temperature.[6–9] The temperature at which the magnetic susceptibility reaches a Curie-Weiss law is theoretically of the order of T_{sf}.[6] A modified Curie-Weiss law, i.e. $\chi(T) = \chi_0 + C/(T + T^*)$, associates T^* with T_{sf} for relatively strong c-f hybridization.[10,11]

Ultrafast time-resolved pump-probe spectroscopy has been recognized as a powerful technique to study the nonequilibrium carrier dynamics in strongly correlated electron materials. In addition to distinguishing different phases in a material by their different relaxation dynamics, it can discern whether one phase coexists or competes with another phase in close proximity,[12,13] giving information on the nature of low energy electronic structure of correlated electron systems, for example, in high-temperature superconductors. Pump-probe experiments have also been performed on actinide compounds, such as the itinerant antiferromagnets $UNiGa_5$ and $UPtGa_5$,[14,15] and the heavy-fermion superconductor $PuCoGa_5$.[16]

The hybridization between the conduction electrons and the localized f electrons also causes a narrow gap to form in the density of states near the Fermi level.[17] This gap, called the hybridization gap, results in a relaxation bottleneck, evidenced by an increase in the relaxation time τ at low temperatures. For example, in heavy fermions such as $YbAgCu_4$ and SmB_6, τ increases monotonically with decreasing temperature.[17]. The temperature dependence of the relaxation amplitude and time were fit using the Rothwarf-Taylor (RT) model. In this paper, we investigate the ultrafast dynamics in three isostructural uranium compounds, UAl_3, UGa_3 and USn_3, using the ultrafast pump-probe technique. The variation in hybridization strength is responsible for the differences in properties of these three isostructural compounds. UAl_3 and USn_3 are categorized as spin-fluctuation systems.[7,18–22] UGa_3 does not behave as a spin fluctuation system, but is an itinerant $5f$ electron antiferromagnet. In fitting the transient change in reflectivity for UAl_3 and USn_3, we needed a two-exponential decay function below T_{sf}, which points to the presence of two relaxation channels below T_{sf}. This arises from the hybridization between f electrons and conduction elec-

trons below T_{sf}. This shows that the ultrafast pump probe technique is sensitive to c-f hybridization in f-electron systems. Our T_{sf} is consistent with that obtained from resistivity and susceptibility measurements. We were also able to fit the temperature dependence of the relaxation amplitude and time using the RT model. For UGa_3, the relaxation time diverges as the temperature approaches the Néel temperature T_N, corresponding to the formation of a spin density wave (SDW) gap near the Fermi level.

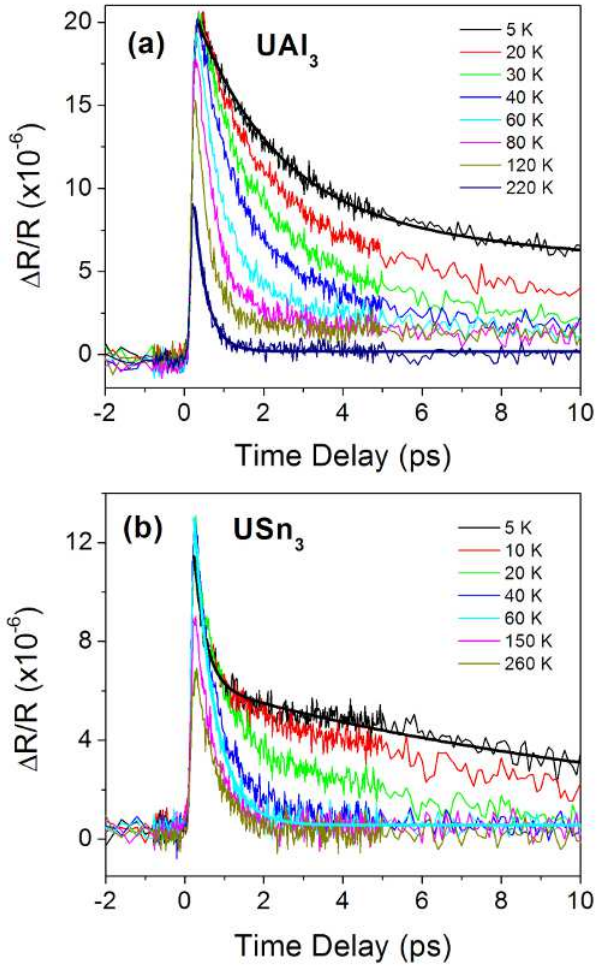

FIG. 1: Transient reflection $\Delta R/R$ versus pump-probe time delay at different temperatures for (a) UAl_3, and (b) USn_3. Thick solid curves denote exponential fits of data, for UAl_3 (at 5 K and 220 K) and USn_3 (at 5 K and 60 K).

II. EXPERIMENTAL SETUP

In our pump-probe experimental setup in reflectance geometry, a Ti:sapphire laser producing sub-100 fs pulses at ≈800 nm (1.55 eV) was used as a source of both pump and probe pulses. The pump and probe pulses were cross polarized. The pump spot diameter was 60 μm and that of probe was 30 μm. The reflected probe beam was focused onto an avalanche photodiode detector. The photoinduced change in reflectivity ($\Delta R/R$) was measured using lock-in detection. In order to minimize noise, the pump beam was modulated at 100 kHz with an acousto-optical modulator. The experiments were performed with an average pump power of 2 mW, giving a pump fluence of ∼1 μJ/cm^2. The probe intensity was approximately ten times lower. Data were taken from 10 K to 300 K. The experiments were performed on single crystals of UX_3 (X = Al, Ga, Sn) grown using standard flux technique, with X used as the flux in each case.[22]

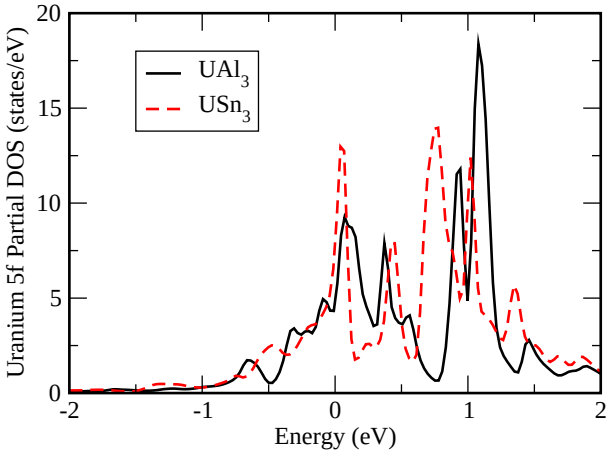

FIG. 2: Uranium $5f$ partial DOS calculated from the LAPW method for UAl_3 and USn_3, in the magnetic unit cell, in the energy range (-2,2) eV. Note the narrower peak width near the Fermi energy (E=0) in USn_3 compared to UAl_3.

III. UAl_3 AND USn_3

In Fig. 1 we show the $\Delta R/R$ at different temperatures for (a) UAl_3 and (b) USn_3, as a function of the time delay between the pump and probe pulses. In both UAl_3 and USn_3, only a fast relaxation of ∼500 fs, which is typical of regular metals, is observed at high temperatures. At low temperatures, an additional slow, positive picosecond relaxation is observed. Data at low temperatures are fitted to the two-exponential decay function $\Delta R/R(t) = A_{fast}(T)\exp(-t/\tau_{fast}) + A_{slow}(T)\exp(-t/\tau_{slow})$. This change from one- to two-exponential decay occurs at a particular crossover temperature — ∼200 K for UAl_3 and ∼50 K for USn_3, suggestive of two relaxation channels below this crossover temperature. These crossover temperatures are of the order of the spin fluctuation temperatures T_{sf} obtained in these compounds from temperature-dependent electrical resistivity and magnetic susceptibility measurements (∼150 K for UAl_3[6,23] and ∼50 K for USn_3[6,24,25]). We thus associate this crossover temperature to the spin fluctuation temperature T_{sf}.

To understand the different characteristic temperatures in UAl_3 and USn_3, we have also performed band

structure calculations in the framework of the density functional theory, by using the WIEN2k linearized augmented plane wave method.[26] A generalized gradient approximation[27] was used to treat exchange and correlation. Spin-orbit coupling was included in a second-variational way. The obtained U partial $5f$ density of states, as shown in Fig. 2, indicates a narrower peak width near the Fermi energy, in USn_3 as compared with UAl_3. In addition, one can see that the splitting between the two major peaks is smaller in USn_3 than in UAl_3. In view of the fact that the spin-orbit coupling is quite local to the U atoms, one would expect the same effect on both USn_3 and UAl_3. A possible explanation for this difference is a smaller hybridization gap in USn_3 compared to UAl_3, due to the weakening of the hybridization in USn_3 — a result of the lattice expansion (a=4.626 Å in USn_3 versus a=4.264 Å in UAl_3).[23] Though conventional band structure calculations underestimate the correlation effect, the trend of smaller coherence energy scale in USn_3 than in UAl_3 should be robust, as has recently been exemplified in other isostructural actinide compounds.[28]

In this context, the two-exponential behavior at low temperature can be explained by the c-f hybridization occurring below T_{sf}. Below T_{sf}, the interaction of partially-filled f shell electrons with conduction electrons lead to the formation of heavy quasiparticles.[29] As the f-electrons are localized above T_{sf}, relaxation occurs through phonon channel only. Hence only a single exponential decay is expected above T_{sf}. When $T < T_{sf}$, the spin fluctuation channel opens up due to hybridization. Electrons now relax via *both* phonon and spin fluctuation channels resulting in a two-exponential decay behavior. Also, a higher T_{sf} value in UAl_3 compared to USn_3 points to a stronger c-f hybridization, which is expected, as c-f hybridization tends to decrease as the size of the non-f atom increases,[3,30] which causes the lattice expansion as we discussed above.

The hybridization between the conduction band and the localized f-levels also results in the formation of a narrow gap in the density of states near the Fermi level, called the hybridization gap. The presence of this gap causes a bottleneck in quasiparticle relaxation, resulting in a divergence of the relaxation time at low temperatures. The temperature dependence of the relaxation amplitude and relaxation time can be quantitively explained by the Rothwarf-Taylor (RT) model. It is a phenomenological model that was used to describe the relaxation of photoexcited superconductors,[31,32] itinerant antiferromagnets[14,15] and heavy-fermion metals,[17] where the presence of a gap in the electronic density of states gives rise to a relaxation bottleneck for carrier relaxation. In heavy fermions, after the initial photo-excitation by a pump pulse, the subsequent fast relaxation due to electron-electron scattering results in excess densities of electron-hole pairs (EHPs) and high-frequency phonons (HFPs). When an EHP with energy $\geq \Delta$ (Δ= hybridization gap) recombines, a HFP is created. The HFPs released in the EHP recombination are trapped within the excited volume and can re-excite EHPs; hence they act as a bottleneck for EHP recombination, and recovery is governed by the decay of the HFP population. The evolution of EHP and HFP populations is described by a set of two coupled nonlinear differential equations.

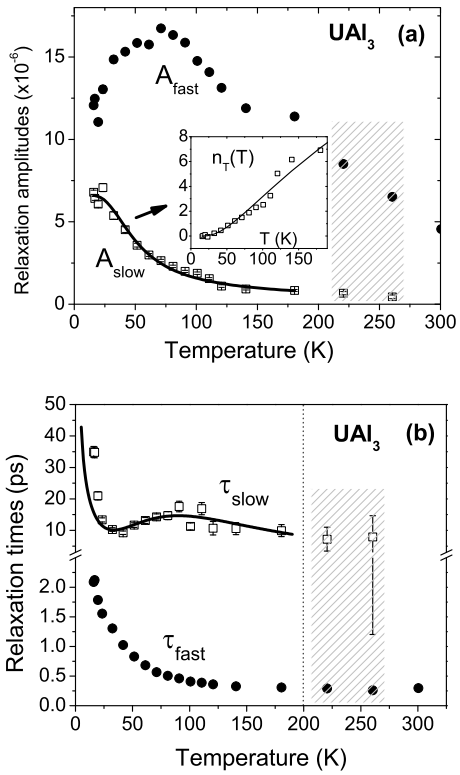

FIG. 3: Temperature dependence of (a) amplitudes and (b) relaxation times for UAl_3. Solid lines are fits to the RT model of the slow component. The shaded regions represent the temperature region above T_{sf} where, though a two-exponential fit is better, a one-exponential fit suffices.

The results of the RT model are as follows:[17,33] from the amplitude $A(T)$, one obtains the density of thermally excited EHPs n_T via the relation

$$n_T(T) \propto \mathcal{A}(T)^{-1} - 1 \qquad (1)$$

where $\mathcal{A}(T)$ is the normalized amplitude ($\mathcal{A}(T) = A(T)/A(T \to 0)$). Then we fit the experimental $n_T(T)$ to the expression[17]

$$n_T(T) \propto \sqrt{T}\exp(-\Delta/T), \qquad (2)$$

where the hybridization gap Δ is temperature independent (or very weakly temperature dependent) and can be obtained from the fitting. Moreover, for a constant pump intensity, the temperature-dependence of n_T also governs the temperature-dependence of τ^{-1}, given by

$$\tau^{-1}(T) = \Gamma[\delta(\beta n_T + 1)^{-1} + 2n_T](\Delta + \alpha T \Delta^4) \qquad (3)$$

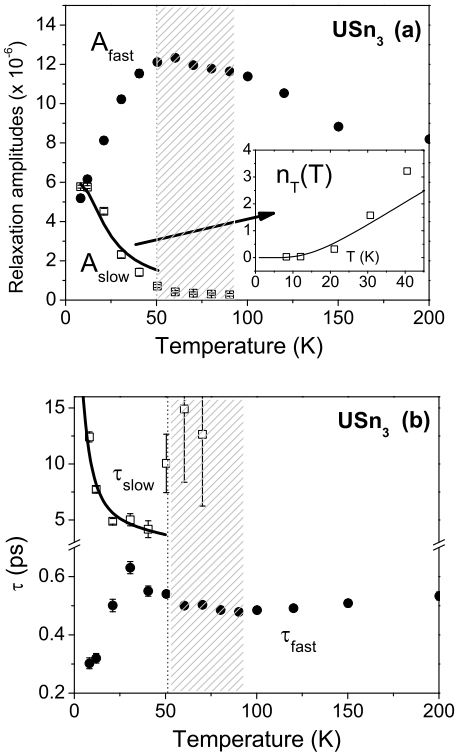

FIG. 4: Temperature dependence of (a) amplitude and (b) relaxation time for USn_3. Solid lines are fits to the RT model of the slow component. The shaded regions represent the temperature region above T_{sf} where, though a two-exponential fit is better, a one-exponential fit suffices.

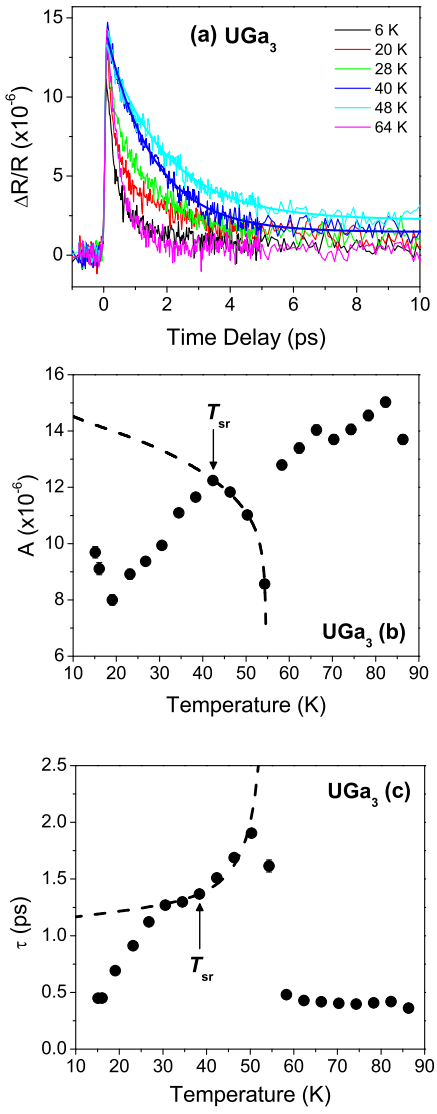

FIG. 5: (a) Photoinduced change in reflectivity $\Delta R/R$ versus pump-probe time delay at different temperatures of UGa_3. Thick blue (cyan) curves denote one-exponential fits of data at T=40 K (48 K). Temperature dependence of (b) amplitude and (c) relaxation time for UGa_3 obtained from one-exponential fits, with dashed lines in (b) and (c) being fits to the RT model from 40 K to T_N.

where Γ, δ, β and α are T-independent fitting parameters. We note that the same type of RT analysis can be made for the quasiparticle scattering off spin fluctuations, when the latter have a spin resonance nature at a finite frequency. Under this condition, spin fluctuations will exhibit a gap-like feature in the integrated spin spectral function.

Since, below T_{sf}, the second relaxation component appears, we attribute it to relaxation across the hybridization gap, and use the RT model to fit the its amplitude and relaxation time below T_{sf} in UAl_3 and USn_3. The inset of Fig. 3(a) shows $n_T(T)$ obtained from $A_{slow}(T)$ using Eq. (1), with the solid line being the fit to Eq. (2), with the fitting parameter $\Delta \approx (230 \pm 10)$ K. The fitted values of $n_T(T)$ are then inserted into Eq. (3) to fit the experimental values of $\tau_{slow}(T)$, shown in Fig. 3(b). Similar fits are also done for USn_3, as shown in Fig. 4, yielding $\Delta \approx (90 \pm 20)$ K. The good fits show that the slow relaxation component in both UAl_3 and USn_3 can be described by assuming EHPs relaxing across the hybridization gap near the Fermi surface. More interestingly, the extracted hybridization gap in UAl_3 is larger than in USn_3, in qualitative agreement with the band structure results. This comparison of hybridization gap is also consistent with that of spin fluctuation energy scale T_{sf} discussed above. Our results show that the ultrafast pump-probe technique is sensitive to the hybridization of f-electron orbitals with the conduction electron orbitals.

Note that, in both UAl_3 and USn_3, there exists a temperature range (indicated by the shaded regions in Figs. 3

and 4), where, though a two-exponential fit is better, a one-exponential fit suffices. The values of τ_{slow}, naturally, have large error bars there, and the values of A_{slow} approach zero. The gradual change in A_{slow} in UAl_3 and USn_3, around T_{sf}, is consistent with T_{sf} being a crossover temperature, rather than a sharp phase transition temperature. T_{sf} is also the temperature below which τ_{fast} starts to rise *gradually*, consistent with that seen in other heavy fermions.[17]

It is worth mentioning that mixed-valence systems exhibit the same behavior as spin-fluctuation systems by having a susceptibility maximum at some crossover temperature (T_{sf} in spin-fluctuation, and T_{max} in mixed-valence). However, the sign of magnetoresistivity (MR) is opposite — negative in spin-fluctuation systems, and positive in mixed-valence systems. For example, in $UCoGa_5$, a normal positive behavior of MR was observed, which the authors used to rule out the possibility of spin fluctuation as a mechanism for the susceptibility maximum, and supports the idea of valence instability in this compound.[34] Since the MR in UAl_3 and USn_3 are positive,[23,25] one might rule out UAl_3 and USn_3 being spin-fluctuation systems as well, though the authors there did not suggest this. Theoretical work that links a negative MR to spin fluctuations was carried out using a self-consistent renormalized spin fluctuation theory[35] — however the theory was developed for weakly ferromagnetic metals, which UAl_3 and USn_3 are obviously not. On the other hand, static (specific heat) and dynamic (spin-lattice relaxation time T_1) properties measured on USn_3, showed that these properties in the heavy-fermion state can be described in a quantitatively consistent way via a spin-fluctuation model, albeit with a temperature-dependent effective Ruderman-Kittel-Kasuya-Yosida (RKKY) interaction, in order to explain the crossover from an incoherent, localized state to a coherent, heavy-fermion state.[36]

Moreover, though the U $5f$ electrons are largely thought to be itinerant/delocalized in character, some degree of localization were seen in certain U compounds. For example, though the $5f$ states of α–U metal and US are largely itinerant, those in USe are localized to a greater extent, whereas those in UTe are almost entirely localized.[37] Electron energy-loss spectroscopy and spin-orbit sum rule analysis showed that the $5f$ states in URu_2Si_2 are moderately localized, though not as much as USe and UTe.[37] However, electronic structure calculation of URu_2Si_2 showed that a completely itinerant picture is sufficient to provide an excellent explanation of the low-temperature data of the paramagnetic and antiferromagnetic phases.[38,39] The itinerant band picture is adequate for the monocarbide UC, and acceptable for the mononitride UN.[40] Furthermore, we note that the fast component of dynamics has a very different temperature dependence of relaxation between UAl_3 and USn_3 (compare Figs. 3(b) and 4(b)). Since this energy scale ($1/\tau_{fast}$) is larger than that involved in the slow dynamics, the understanding of the fast dynamics may help identify the relevance of spin fluctuations, mixed valence, and dual nature in these heavy fermion systems — how these different descriptions can explain the crossover from a single- to double-exponential relaxation behavior in our pump-probe data, requires further theoretical and experimental work.

IV. UGa_3

We now turn to the relaxation dynamics of UGa_3. UGa_3 is not a spin fluctuation system — it is a SDW system with Néel temperature T_N=65 K. It is a moderate heavy fermion with Sommerfeld coefficient 52 $mJ/K^2.mol$,[18] and is reported to follow a modified Curie-Weiss law behavior[41] with T^*=2080 K which is indicative of strong hybridization in this compound. The $5f$ electrons in UGa_3 can be considered itinerant because of the large hybridization of $5f$ orbitals with conduction electron orbitals. Neutron scattering[42] and resistivity[4,41] data revealed a antiferromagnetic transition at ∼70 K. Kaczorowski[43] summarized the properties of UGa_3, and found it to fulfil all the main criteria for itinerant magnetism. Further evidence for the itinerancy of $5f$ electrons in UGa_3 comes from data of angular correlation of the electron-positron annihilation radiation, and supported by electronic structure calculations within the local density approximation.[26,44]

The photoinduced change in reflectivity, as shown in Fig. 5(a), can be fitted with a single exponential decay $\Delta R/R(t) = A(T)\exp(-t/\tau)$. The extracted relaxation amplitude $A(T)$ and time $\tau(T)$ are shown in Fig. 5(b) and Fig. 5(c), respectively. Upon entering the SDW phase, $A(T)$ increases with decreasing temperature. However, instead of monotonically increasing as in UAl_3 and USn_3, $A(T)$ now attains a maximum at ∼40 K and starts decreasing with decreasing temperature (see Fig. 5(b)). Concurrently, τ exhibits a quasi-divergence at T_N, consistent with that observed in itinerant antiferromagnets $UNiGa_5$ and $UPtGa_5$, where the opening up of the SDW gap causes a bottleneck in quasiparticle relaxation.[14,15] In contrast to $UNiGa_5$ and $UPtGa_5$, however, where τ increases with decreasing temperature at low temperatures, τ in UGa_3 shows a (1) shoulder (or change in curvature) at 40 K, and (2) decrease with decreasing temperature. An anomaly at a spin-reorientation temperature T_{sr}=40 K has been reported in other measurements of UGa_3, whether in the presence of a magnetic field (nuclear magnetic resonance, neutron scattering, magnetic susceptibility, Mössbauer),[45–50] or in the absence of a magnetic field (thermal conductivity and neutron scattering).[45,46,51] This anomaly has been associated with a reorientation of the ordered magnetic moments,[46,47,49–51] which induces strong modifications of the uranium $5f$ orbitals.[48] The magnetic moments, oriented along the [110] axis below 40 K, reorient into [111] direction at 40 K.[43,51,52] The fact that the transition is observed in the absence of magnetic field is an indication that the

bump we see at 40 K in our pump probe measurement is not an artifact, but corresponds to the moment reorientation as has been reported in other measurements mentioned above.

We use the model proposed by Kabanov *et al.*[53] to analyze the temperature dependence of A. The temperature-dependence of the relaxation amplitude in the SDW state for an isotropic temperature-*dependent* gap $\Delta_{SDW}(T)$ is given by (writing $\Delta_{SDW}(T)$ as $\Delta(T)$)

$$A(T) = \frac{\epsilon_I/(\Delta(T) + k_B T/2)}{1 + \zeta\sqrt{\frac{2k_B T}{\pi\Delta(T)}}\exp[-\Delta(T)/k_B T]}, \qquad (4)$$

where ϵ_I the pump laser intensity per unit cell, ζ is a constant, and $\Delta(T)$ obeys a weak-coupling BCS temperature dependence. The above expression for $A(T)$ describes a reduction in the photoexcited quasiparticle density with increase in temperature, due to the decrease in gap energy and corresponding enhanced phonon emission during the initial relaxation. A good fit between the experimental $A(T)$ and Eq. (4) can only be made from T_N down to ∼40 K, where T_N=55 K is a fitting parameter. In the SDW state ($T < T_N$), the temperature-dependence of τ cab be obtained from Eq. (3), but can be written in the alternative form (writing $\Delta_{SDW}(T)$ as $\Delta(T)$)[13]

$$\tau^{-1}(T) = \Gamma\{\delta A(T) + \eta\sqrt{\Delta(T)T}\exp[-\Delta(T)/T]\} \times \left[\Delta(T) + \alpha T\Delta(T)^4\right]. \qquad (5)$$

The fit of $\tau(T)$ to Eq. (5) is shown in Fig. 5(c). Once again, a good fit is obtained only from T_N to ∼30 K, close to T_{sr}. Below T_{sr}, the fit deviates from the experimental data, consistent with the existence of another transition at T_{sr}.

V. CONCLUSION

We have performed time-resolved photoinduced change in reflectivity measurements on three isostructural uranium compounds — UAl_3, UGa_3 and USn_3. The values of T_{sf}, a measure of the degree of hybridization, in UAl_3 and USn_3, are consistent with data from other measurements. Our fit of the slow component to the Rothwarf-Taylor model shows that the slow component can be described by assuming electron-hole pairs relaxing across the hybridization gap. We have thus shown the pump probe technique to be sensitive to c-f hybridization. Our data on UGa_3 is consistent with the formation of a SDW gap at T_N=60 K, and a reorientation of magnetic moments at T_{sr}=40 K.

VI. ACKNOWLEDGEMENTS

E.E.M.C. acknowledges support from G. T. Seaborg Postdoctoral Fellowship, the Singapore Ministry of Education Academic Research Fund Tier 2 (ARC23/08), as well as the National Research Foundation Competitive Research Programme (NRF-CRP4-2008-04). Work at Los Alamos was supported by the U.S. DOE at LANL under Contract No. DE-AC52-06NA25396, the U.S. DOE Office of Basic Energy Sciences, and the LDRD Program at LANL. The electronic structure calculations were performed on a computer cluster at the Center for Integrated Nanotechnologies, a U.S. DOE Office of Basic Energy Sciences user facility.

[1] J. M. Fournier and R. Troć, *Handbook on the Physics and Chemistry of the Actinides*, vol. 2 (North-Holland, Amsterdam, 1985).
[2] H. H. Hill, in *Plutonium and other Actinides*, edited by W. N. Miner (Nuclear Materials Sciences, AIME, New York, 1970), vol. 17, pp. 2–17.
[3] D. D. Koelling, B. D. Dunlap, and G. W. Crabtree, Phys. Rev. B **31**, 4966 (1985).
[4] H. R. Ott, F. Hulliger, H. Rudigier, and Z. Fisk, Phys. Rev. B **31**, 1329 (1985).
[5] A. J. Arko, M. B. Brodsky, and W. J. Nellis, Phys. Rev. B **5**, 4564 (1972).
[6] R. Jullien and B. Coqblin, J. Low Temp. Phys. **22**, 437 (1976).
[7] K. H. J. Buschow and H. J. van Daal, AIP Conference Proceedings **5**, 1464 (1972).
[8] R. Jullien, M. T. Béal-Monod, and B. Coqblin, Phys. Rev. Lett. **30**, 1057 (1973).
[9] R. Jullien, M. T. Béal-Monod, and B. Coqblin, Phys. Rev. B **9**, 1441 (1974).
[10] C. L. Lin, L. W. Zhou, J. E. Crow, and R. P. Guertin, J. Appl. Phys. **57**, 3146 (1985).
[11] T. Yuen, Y. Gao, I. Perez, and J. E. Crow, J. Appl. Phys. **67**, 4827 (1990).
[12] E. E. M. Chia, J.-X. Zhu, D. Talbayev, R. D. Averitt, A. J. Taylor, K. H. Oh, I. S. Jo, and S. I. Lee, Phys. Rev. Lett. **99**, 147008 (2007).
[13] S. K. Nair, X. Q. Zou, E. E. M. Chia, J.-X. Zhu, C. Panagopoulos, S. Ishida, and S. Uchida, Phys. Rev. B **82**, 212503 (2010).
[14] E. E. M. Chia, J.-X. Zhu, H. J. Lee, N. Hur, N. O. Moreno, E. D. Bauer, T. Durakiewicz, R. D. Averitt, J. L. Sarrao, and A. J. Taylor, Phys. Rev. B **74**, 140409 (2006).
[15] E. E. M. Chia, J.-X. Zhu, D. Talbayev, H. J. Lee, N.Hur, N. O. Moreno, R. D. Averitt, J. L. Sarrao, and A. J. Taylor, Phys. Rev. B **84**, 174412 (2011).
[16] D. Talbayev, K. S. Burch, E. E. M. Chia, S. A. Trugman, J.-X. Zhu, E. D. Bauer, J. A. Kennison, J. N. Mitchell, J. Thompson, J. L. Sarrao, et al., Phys. Rev. Lett. **104**, 227002 (2010).
[17] J. Demsar, J. L. Sarrao, and A. J. Taylor, J. Phys.: Condens. Matter **18**, R281 (2006).

[18] M. H. Van Maaren, H. J. Van Daal, K. H. J. Buschow, and C. J. Schinkel, Solid State Commun. **14**, 145 (1974).

[19] I. Lupsa, P. Lucaci, and E. Burzo, J. Alloys Compd. **204**, 247 (1994).

[20] I. Lupsa, E. Burzo, and P. Lucaci, J. Magn. Magn. Mater. **157 & 158**, 696 (1996).

[21] M. R. Norman, S. D. Bader, and H. A. Kierstead, Phys. Rev. B **33**, 8035 (1986).

[22] A. L. Cornelius, A. J. Arko, J. L. Sarrao, J. D. Thompson, M. F. Hundley, C. H. Booth, N. Harrison, and P. M. Oppeneer, Phys. Rev. B **59**, 14473 (1999).

[23] D. Aoki, N. Watanabe, Y. Inada, R. Settai, K. Sugiyama, H. Harima, T. Inoue, K. Kindo, E. Yamamoto, Y. Haga, et al., J. Phys. Soc. Jpn. **69**, 2609 (2000).

[24] M. Loewenhaupt and C. K. Loong, Phys. Rev. B **41**, 9294 (1990).

[25] K. Sugiyama, T. Iizuka, et al., J. Phys. Soc. Jpn. **71**, 326 (2002).

[26] P. Blaha, K. Schwarz, G. K. H. Madsen, D. Kvasnicka, and J. Luitz, *WIEN2k, An Augmented Plane Wave Plus Local Orbitals Program for CalculatingCrystal Properties* (Vienna University of Technology, Austria, 2001).

[27] J. P. Perdew, K. Burke, and M. Ernzerhof, Phys. Rev. Lett. **77**, 3865 (1996).

[28] J.-X. Zhu, P. H. Tobash, E. D. Bauer, F. Ronning, B. L. Scott, K. Haule, G. Kotliar, R. C. Albers, and J. M. Wills, Europhys. Lett. **97**, 57001 (2012).

[29] A. I. Lobad, A. J. Taylor, J. L. Sarrao, and S. A. Trugman, in *Quantum Electronics and Laser Science Conference, 2000. (QELS 2000). TechnicalDigest* (2000), pp. 159 – 160.

[30] A. J. Arko and D. D. Koelling, Phys. Rev. B **17**, 3104 (1978).

[31] A. Rothwarf and B. N. Taylor, Phys. Rev. Lett. **19**, 27 (1967).

[32] J. Demsar, R. D. Averitt, A. J. Taylor, V. V. Kabanov, W. N.Kang, H. J. Kim, E. M. Choi, and S. I. Lee, Phys. Rev. Lett. **91**, 267002 (2003).

[33] V. V. Kabanov, J. Demsar, and D. Mihailovic, Phys. Rev. Lett. **95**, 147002 (2005).

[34] R. Troć, Z. Bukowski, C. Sulkowski, H. Misiorek, J. A. Morkowski, A. Szajek, and G. Chelkowska, Phys. Rev. B **70**, 184443 (2004).

[35] K. Ueda, Solid State Commun **965-968**, 965 (1976).

[36] S. Kambe, H. Sakai, Y. Tokunaga, T. D. Matsuda, Y. Haga, H. Chudo, and R. E. Walstedt, Phys. Rev. B **77**, 134418 (2008).

[37] J. R. Jeffries, K. T. Moore, N. P. Butch, and M. B. Maple, Phys. Rev. B **82**, 033103 (2010).

[38] P. M. Oppeneer, J. Rusz, S. Elgazzar, M. T. Suzuki, T. Durakiewicz, and J. A. Mydosh, Phys. Rev. B **82**, 205103 (2010).

[39] G. L. Dakovski, Y. Li, S. M. Gilbertson, G. Rodriguez, A. V. Balatsky, J.-X. Zhu, K. Gofryk, E. D. Bauer, P. H. Tobash, A. Taylor, et al., Phys. Rev. B **84**, 161103 (2011).

[40] L. Petit, A. Svane, Z. Szotek, W. M. Temmerman, and G. M. Stocks, Phys. Rev. B **80**, 045124 (2009).

[41] L. W. Zhou, C. S. Jee, C. L. Lin, J. E. Crow, S. Bloom, and R. P. Guertin, J. Appl. Phys. **61**, 3377 (1987).

[42] A. Lawson, A. Williams, J. Smith, P. Seeger, J. Goldstone, JAand O'Rourke, and Z. Fisk, J. Magn. Magn. Mater. **50**, 83 (1985), ISSN 0304-8853.

[43] D. Kaczorowski, J. Phys. Soc. Jpn. **75S**, 68 (2006).

[44] J. Rusz, M. Biasini, and A. Czopnik, Phys. Rev. Lett. **93**, 156405 (2004).

[45] D. Kaczorowski, P. W. Klamut, A. Czopnik, and A. Jeżowski, J. Magn. Magn. Mater. **177**, 41 (1998).

[46] P. Dervenagas, D. Kaczorowski, F. Bourdarot, P. Burlet, A. Czopnik, and G. H. Lander, Physica B **269**, 368 (1999).

[47] S. Kambe, H. Kato, H. Sakai, R. E. Walstedt, Y. Haga, D. Aoki, and Y. Ônuki, Physica B **312-313**, 902 (2002).

[48] S. Kambe, H. Kato, H. Sakai, Y. Tokunaga, R. E. Walstedt, Y. Haga, H. Yasuoka, and D. Aoki, Physica B **329**, 614 (2003).

[49] S. Kambe, R. E. Walstedt, H. Sakai, Y. Tokunaga, T. D. Matsuda, Y. Haga, and Y. Ônuki, Phys. Rev. B **72**, 184437 (2005).

[50] J. P. Sanchez, P. Vulliet, M. M. Abd-Elmeguid, and D. Kaczorowski, Phys. Rev. B **62**, 3839 (2000).

[51] M. Nakamura, Y. Koike, N. Metoki, K. Kakurai, Y. Haga, G. H. Lander, D. Aoki, and Y. Ônuki, J. Phys. Chem. Solids **63**, 1193 (2002).

[52] M. Nakamura, T. D. Matsuda, K. Kakurai, G. H. Lander, S. Kawarazaki, and Y. Ônuki, J. Phys.: Condens. Matter **15**, S1997 (2003).

[53] V. V. Kabanov, J. Demsar, B. Podobnik, and D. Mihailovic, Phys. Rev. B **59**, 1497 (1999).